J Solid State Electrochem (2011) 15:285–291
DOI 10.1007/s10008-010-1096-7

ORIGINAL PAPER

Comments on charge density waves

John B. Goodenough

Received: 30 April 2010 / Revised: 6 May 2010 / Accepted: 9 May 2010 / Published online: 28 May 2010

Abstract Charge density waves (CDWs) in transition-metal compounds are shown to be a consequence of the first-order character of the crossover from localized to itinerant *d*-electron behavior; they are formed as this crossover is approached from either the localized-electron or the itinerant-electron side. Opening of a gap at the Fermi energy by changing the periodicity of the electron potential energy is a description that is only applicable on the approach from the itinerant-electron side. At crossover, single-valent transition-metal compounds with metal–metal *d*-electron bonding form cation clusters in which *d*-electrons are confined to molecular orbitals; normally, the individual bonds of a cluster are electron-pair bonds. However, in $Zn[V_2]O_4$, orbital ordering of a localized *3d*-electron in an *xy*-orbital lowers the V–V separation in [011] and [101] chains sufficiently that the $yz \pm izx$ orbitals approach crossover from the localized-electron side. To resolve the magnetic frustration associated with the antiferromagnetic coupling between the localized spins in neighboring *xy* orbitals, the $yz \pm izx$ electrons become confined to one-electron bonds in a zigzag chain rather than an electron-pair bond within a dimer. The itinerant *d*-electrons of the zigzag chains are spin-polarized by intra-atomic exchange with *xy*-orbital spins. At crossover, compounds with cation–anion–cation bonding segregate into cations of an anion complex and cations with localized-electron spins; these segregations commonly result in a disproportionation electron transfer between cations that result in a static "negative-U" CDW in either single-valent or mixed-valent systems, but the perovskite $HoNiO_3$ demonstrates that this electron transfer does not always occur. The insertion of interstitial O_i atoms in the $La_2CuO_{4+\delta}$ system allows monitoring of the formation of a dynamic phase segregation into mobile multihole polarons in a hole-free matrix that order into a thermodynamically distinct superconductive phase. The polarons may either order into pinned metallic stripes or as two-hole, two-electron bosonic polarons that become pinned to phonons in a superconductive phase that masks a quantum critical point.

Keywords Insertion compounds · Localized-itinerant *d*-electron transition · Copper-oxide superconductivity

J. B. Goodenough (✉)
Texas Materials Institute, Mechanical Engineering, ETC 9.102,
University of Texas at Austin,
1 University Station, C2200,
Austin, TX 78712, USA
e-mail: jgoodenough@mail.utexas.edu

Introduction

Robert Schöllhorn pioneered the field of intercalation chemistry and insertion compounds [1]. This chemistry is now the basis for the design of a solid cathode for a rechargeable Li-ion battery [2]. The battery cathodes consist of a transition-metal oxide-host structure having an interconnected interstitial space into which Li^+ ions are inserted; on discharge, they are charge-compensated by electrons from the anode that enter the *d* states of the transition-metal atoms. The energies of the cation *d* states are either located between the occupied anion *p* bands and an empty cation *s* band or have strongly hybridized O-2*p* and cation *d* states of *d* orbital symmetry with the Fermi energy pinned at the top of the O-2*p* bands. The *d* states of the transition-metal M atoms may be localized or itinerant depending on the relative strengths of the intra-atomic versus interatomic interactions. This competition makes it possible to explore the transition from localized to itinerant behavior of the *d*-electrons, and guest-ion insertion gives us the ability to explore this transition in a mixed-valent host without doping the host structure with substitutional ions or ion vacancies.

In this note, I point out that the phenomenon of charge density wave (CDW) formation is a consequence of the first-order character of the transition from localized to itinerant electronic behavior. In single-valent systems, a static CDW may be formed on approaching the transition from either the localized-electron side or the itinerant-electron side; the former approach results in a semiconductor–insulator transition, the latter in a metal-insulator transition. Only the latter can be described by a model of Fermi surface nesting. A static CDW can be described as a single crystallographic phase, but it contains ordered atomic clusters in which the itinerant character of the electrons is confined to molecular orbitals of a cluster. In a mixed-valent system, inability to form an ordered array of atomic clusters may lead to a spinodal, dynamic phase segregation with the option of forming a traveling CDW at lowest temperatures.

Concept foundations

Single-valent compounds

Single-valent host structures containing localized *d*-electron manifolds have the energies of successive manifolds separated by a finite gap, the effective intra-atomic energy [3]

$$U_{\text{eff}} = U + \begin{cases} o \\ \Delta_c \\ \Delta_{\text{ex}} \end{cases} \tag{1}$$

where U is the Hubbard screened electrostatic on-site energy associated with adding an electron to a multielectron manifold and the energies Δ_c and Δ_{ex} are any intra-atomic ligand-field splittings or Hund exchange-field splitting that must also be overcome. (Any spin-orbit splitting $\lambda \mathbf{L}\bullet\mathbf{S}$ is included in Δ_c.) The spin-independent expectation integral for an interatomic charge transfer is

$$b_{ij} = \left(\phi_i, H'\phi_j\right) = \varepsilon_{ij}\left(\phi_i, \phi_j\right) \tag{2}$$

where ε_{ij} is a one-electron energy depending on the magnitude of the perturbation H' of the atomic potential by the neighboring atoms; $(\phi_{\text{i}}, \phi_{\text{j}})$ is the overlap integral for the *d*-electron ligand-field *d*-like wave functions ϕ_{i} and ϕ_{j} on neighboring like atoms in energy-equivalent lattice sites. The anion hybridization with the cation *d* orbitals is included in the ligand-field wave functions ϕ. Splitting of localized d^n and d^{n+1} manifolds by U_{eff} retains localized cation spins, but there is an interatomic spin–spin interaction energy that is treated in higher-order perturbation theory. The interaction energy between half-filled *d* orbitals, for example, is [4]

$$\Delta E = -2b^2/\left(4S^2 U_{\text{eff}}\right) \tag{3}$$

where S is the cation spin and b is the b_{ij} for nearest neighbors and U_{eff} is given by Eq. 1.

On the other hand, single-valent host structures containing partially filled bands of one-electron itinerant-electron states are metallic and, in the absence of localized spins, Pauli paramagnetic. In tight-binding theory, the width of a narrow *d* band is

$$W_b \approx 2zb \tag{4}$$

where z is the number of nearest neighbors.

Charge transfer between like atoms increases the screening of localized electrons from the nuclear charge. The greater the screening, the smaller the energy U, and a smaller U increases the charge transfer. This feedback results in a first-order transition [5]. Furthermore, from the Virial Theorem for central force fields, it follows [6] that the volume of the phase with itinerant antibonding *d*-electrons is smaller than the phase with localized antibonding *d*-electrons. (The *d*-electrons are antibonding with respect to the M–O interactions.)

Mixed-valent systems

Where the host of an insertion compound undergoes a transition from localized to itinerant electronic behavior with increasing concentration of the guest ion, it is possible to monitor the evolution of physical properties on crossing from the localized to the itinerant side of the transition.

For localized electrons, the many-electron manifolds may be described as redox couples. A mixed-valent system has its Fermi energy within the couple, and the formation of dielectric polarons lifts the energies of the empty states of a couple above those of the filled states by a polaron energy ε_{p}. A small dielectric polaron corresponds to confinement of the mobile charge to a single ion with a hopping time $\tau_h \approx \text{h}/W_b > \omega_R^{-1}$ for a real charge transfer between like atoms and a bandwidth W_b; ω_R^{-1} is the period of the optical-mode lattice vibration that would trap the charge carrier at a single site. The motion of the small-polaron charge carrier and its associated local site distortion is diffusive with a motional enthalpy $\Delta H_m \approx \varepsilon_p$.

As the intersite overlap integral $(\phi_{\text{i}}, \phi_{\text{j}})$ increases in an oxide, the polaron energy ε_p decreases to where it may allow formation of a single-electron molecular orbital that includes a cluster of nearest like cation neighbors before the charge carriers are rendered itinerant. The motional enthalpy of the large single-charge polaron would be strongly reduced [7]. At larger concentrations, larger single-charge polarons must interact to form either an itinerant-electron

second phase or mobile multicharge polarons in a single phase that may either remain disordered or order into a CDW. In the absence of pinning of the multicharge polarons into a static CDW by a lattice distortion, a multicharge polaron would have a motional enthalpy $\Delta H_m=0$, and ordering into a traveling CDW may lead to superconductivity if the multicharge polarons contain two spin-paired charge carriers. Four open questions are yet to be resolved: (1) Does formation of multicharge polarons occur as a first-order phase change? (2) Does the electrostatic coulomb repulsion between two-charge polarons keep them from coalescing into an itinerant-electron second phase? (3) Does ordering of two-electron plus two-hole multielectron polarons into a CDW lead to itinerant-electron stripes separated by single-valent stripes in a static CDW pinned by a lattice distortion or to spin-paired mobile bipolarons that are superconductive? (4) Does failure to order the multielectron polarons into either a static or a traveling CDW lead to quantum critical point (QCP) behavior?

Experimental examples

VO_2

Morin [8] was the first to identify a first-order metal–insulator transition in VO_2 on cooling through T_t=67 °C. The high-temperature tetragonal rutile structure has *c*-axis chains of edge-shared $VO_{6/3}$ octahedra with a V–V separation close to the critical separation for a transition from localized to itinerant electronic behavior. The electronic conductivity is essentially isotropic in this phase. On cooling through the transition temperature T_t, the structure changes to monoclinic as a result of *c*-axis pairing of the V(IV):$3d^1$ atoms into spin-paired dimers; ordering of the electrons into the V–V bonds of a dimer allows ferroic displacements of the V(IV) ions perpendicular to the *c*-axis to rock the dimers by formation of V=O vanadyl ions with the oxide ions that do not bridge the *c*-axis V–V bonds [9, 10]. This transition represents an ordered segregation of itinerant 3*d*-electrons in the rutile phase of single-valent VO_2 into molecular-orbital electrons confined to V–V clusters.

Since the formation of the CDW in VO_2 occurs at a metal–insulator transition in which dimers form in 1D chains, theorists chose to describe this phenomenon as a Peierls distortion in which an energy gap is opened at E_F in a half-filled 1D itinerant-electron band by a doubling of the periodicity of the *c*-axis periodic potential [5, 11]. This formation led, in turn, to the concept of 2D CDW formation as a result of Fermi surface nesting [12]. However, application of this concept to describe 2D cation clustering can be shown to be unable to explain clustering where it occurs below a semiconductor–insulator transition in a single-valent system. Moreover, since opening of a gap in an itinerant-electron energy band by atomic displacements only influences the states near the Brillouin zone boundary, the concept can only be applied where the bandwidth is reduced to a $W_b \approx U_{eff}$ where the transition to a localized-electron regime is approached.

$LiVO_2$

Bongers [13] first demonstrated a first-order transition in $LiVO_2$ from a temperature-dependent paramagnetic susceptibility above $T_t \approx 90$ °C to a small susceptibility below T_t. The structure of high-temperature $LiVO_2$ consists of sheets of edge-shared $VO_{6/3}$ octahedra alternating with Li^+ ions in the octahedral sites between the sheets. The V(III):$3d^2$ and Li^+ ions occupy alternating (111) planes of a face-centered cubic array of oxide ions. Below T_t, the vanadium ions form triangular clusters in which electron-pair bonds are formed in each V–V bond of the cluster [14] rather than molecular orbitals of a V_3 trimer. This case represents a semiconductor to metal transition on the approach to the insulator to metal transition from the localized-electron side; Fermi surface nesting is not applicable to describe this transition.

The $A[V_2]O_4$ spinels

The $A[V_2]O_4$ spinels provide a further test of the conclusion that cation clustering in a single-valent compound may occur on the approach to the crossover from localized to itinerant electronic behavior from the localized-electron side.

From the metal–insulator transitions in VO_2 and V_2O_3 as well as the transition in $LiVO_2$, I had estimated that the critical V–V separation for the crossover from localized to itinerant electronic behavior would be about 2.94 Å for V(III) in a single-valent oxide [15]. Therefore, in 1964, a series of $A[V_2]O_4$ spinels was prepared in an attempt to find the crossover in a family of single-valent isostructural V(III) oxides in which only nearest-neighbor interactions are across shared octahedral-site edges as in $LiVO_2$ [16]. By decreasing the size of the tetrahedral-site A cation, it was possible to decrease the room temperature V–V separation from 3.074 Å in $Cd[V_2]O_4$ to 2.973 Å in $Zn[V_2]O_4$ and 2.972 Å in $Co[V_2]O_4$. All the $A[V_2]O_4$ spinels contained localized electrons on the V(III) ions at room temperature. Since I had accepted the idea that a CDW, and therefore cation clustering, would only occur on the approach to crossover from the itinerant-electron side, I was frustrated by our inability to obtain a metallic $A[V_2]O_4$ spinel.

Recently, Pardo et al. [17] have shown that, below room temperature, $Zn[V_2]O_4$ undergoes a first-order transition to an antiferromagnetic phase in which V–V dimers are formed along [101] and [011] V–V chains of the spinel framework; since each V atom has two V–V interactions in such chains, the resulting lattice distortion leaves zigzag V–V chains having a V–V separation of 2.92 Å separated from one another by a V–V distance of 3.01 Å. The antiferromagnetic order of the distorted phase shows antiferromagnetic coupling in the (001) planes, ferromagnetic coupling in the zigzag chains with shorter V–V bonds, and antiferromagnetic interactions between the zigzag chains. This magnetic configuration can be rationalized by an ordering of one localized *d*-electron in the *xy*-orbital in the (001) basal plane, which leaves the $yz \pm izx$ orbitals only one-quarter-filled with an unquenched orbital angular momentum. A one-quarter-filled pair of degenerate orbitals would give rise to ferromagnetic coupling along the *c*-axis, but ferromagnetic coupling along the *c*-axis is frustrated by the strong antiferromagnetic coupling in the (001) planes. Dimerization resolves this frustration by confining the ferromagnetic coupling to zigzag chains with the shorter 2.92 Å V–V separation, which allows the weaker interaction across the 3.01 Å V–V separation to be forced to be antiferromagnetic by the stronger interactions in the (001) planes [18]. In this case, the intra-atomic spin–spin coupling to the localized *xy*-orbital induces a localized spin from the itinerant electrons in the zigzag dimer chains having a V–V separation less than the estimated critical V–V separation of 2.94 Å for V(III) oxides; this intra-atomic spin–spin interaction and the single-electron character of the bond prevents a greater shortening of the V–V bond within a ferromagnetic chain. The distortion lifts the degeneracy of the *yz* and *zx* orbitals on a V atom, which suppresses the orbital angular momentum. Nevertheless, the observation of dimer formation in a magnetic insulator, even if it is to relieve an interatomic magnetic interaction frustration, shows that a cation clustering instability can occur on the approach to crossover from localized to itinerant electronic behavior from the localized-electron side. In the case of $Zn[V_2]O_4$, ordering of a localized electron into the *xy*-orbital distorts the lattice from cubic to tetragonal ($c/a<1$), which reduces the V–V separation in the [110] and [101] chains to near the critical separation R_c estimated to be in the interval $2.92\ \text{Å} < R_c < 2.97\ \text{Å}$. Dimerization signals a phase separation into itinerant *yz*, *zx* electrons confined to the dimer zigzag chains and localized *xy* electrons in the (001) planes.

The $RNiO_3$ perovskite family

The perovskite structure allows monitoring of the transition from localized to itinerant *d*-electron behavior as a result of changing the strength of the M–O–M interactions [19]. For example, the $RNiO_3$ family changes from metallic in $LaNiO_3$ to an antiferromagnetic insulator with decreasing size of the R^{3+} ion. A localized low-spin Ni(III):t^6e^1 configuration is Jahn-Teller active with a twofold *e*-orbital degeneracy. However, $LaNiO_3$ undergoes a distortion to rhombohedral symmetry $\left(R\bar{3}c\right)$, which is incompatible with removal of the degeneracy, and the narrow Ni(III):$t^6\sigma^{*1}$ state contains a narrow, quarter-filled σ* band of *e*-orbital parentage; $LaNiO_3$ remains metallic without becoming ferromagnetic to lowest temperatures. However, on reducing the size of the R^{3+} ion, the lattice distorts to orthorhombic (*Pbnm*) symmetry. With decreasing temperature, the orthorhombic perovskites undergo a first-order transition from a metal to an insulator below a T_{IM}; antiferromagnetic order occurs at a $T_N \leq T_{IM}$ [20]. The transition at T_{IM} is characterized by cooperative oxygen displacements that create alternating $NiO_{6/3}$ octahedra with short and long Ni–O bonds [21]. Where the interactions between the transition-metal cations is across a bridging oxygen, it is not cation clustering that occurs, but a cation–anion clustering in which stronger covalent bonding is found in the $NiO_{6/2}$ octahedra with shorter Ni–O bonds; the stronger covalent bonding creates σ-bonding Ni-3d, O-2p hybridized molecular orbitals spread out over the $NiO_{6/2}$ cluster to form a polyanion while leaving localized *e* electrons on the Ni(III) having longer Ni–O bonds. This situation leaves an ambiguity. Do the oxygen displacements signal a disproportionation of the Ni(III) into Ni(II) and Ni(IV) ions, which would remove the orbital degeneracy, or do the valence states remain Ni(III) with a Jahn-Teller distortion removing the *e*-orbital degeneracy on the site with longer Ni–O bonds? In $HoNiO_3$, this issue was resolved in favor of retention of the Ni(III) valence states by the observation of a large Jahn-Teller distortion of the site with the longer average Ni–O bond length [20]; but for larger R^{3+} ions, a disproportionation reaction may occur.

Observation of a larger average Ni–O bond length in the insulator phase than the metallic phase invited exploration of the pressure dependence of the Néel temperature $T_N = T_{IM}$, where T_{IM} is an insulator–metal transition temperature, in $PrNiO_3$ [22]. It was shown that pressure reduces $T_N = T_{IM}$ until a first-order transition to a QCP phase occurs below about 40 K.

Mixed-valent $La_2CuO_{4+\delta}$

The parent compound La_2CuO_4 of the $La_{2-x}Sr_xCuO_4$ superconductors is an antiferromagnetic insulator. At high temperatures, it has the tetragonal (I4/mmm) structure of K_2NiF_4; two LaO (001) sheets form a rock-salt layer that alternates with CuO_2 sheets containing 180° Cu–O–Cu bonds. At room temperature, the equi-

librium (A–O) and (Cu–O) bond lengths give a tolerance factor $t \equiv (La-O)/\sqrt{2}(Cu-O)$, which places the CuO_2 sheets under compression and the $(LaO)_2$ layers under tension. These internal stresses manifest themselves in four ways: (1) An exceptionally large, tetragonal ($c/a>1$) distortion of the CuO_6 octahedra in the tetragonal phase signals an ordering of the hole in the Cu(II) 3d shell into x^2-y^2 orbitals, which removes one Cu–O antibonding electron per Cu atom from the CuO_2 sheets. (2) A cooperative rotation of the CuO_6 octahedra about a $[1\bar{1}0]$ axis reduces the Cu–O–Cu bond angle from 180° below a T_t to distort La_2CuO_4 to orthorhombic *Bmab* symmetry. (3) On slow cooling in air, extra oxygen is inserted between the two LaO sheets of the $(LaO)_2$ layers into sites tetrahedrally coordinated by La^{3+} ions. The interstitial oxygen atoms O_i relieve the tensile stress in the $(LaO)_2$ layers and, by capturing electrons from the x^2-y^2 orbitals of the CuO_2 sheets, they also relieve the compressive stress on the CuO_2 sheets. As a result, T_t decreases with increasing concentration δ per formula unit of O_i atoms in $La_2CuO_{4+\delta}$ until the O_i atoms form a new phase, which is thought to be due to O_i ordering, at a $\delta \geq \delta_0$. (4) La_2CuO_4 cannot be doped n-type, but it is readily doped p-type. Substitution of a larger Sr^{2+} for a La^{3+} ion in $La_{2-x}Sr_xCuO_4$ relieves the tensile stress in the $(LaO)_2$ layers; oxidation of the CuO_2 sheets to compensate for the charge change removes antibonding x^2-y^2 electrons from the CuO_2 sheets to relieve the compressive stress. As a result, T_t decreases with increasing δ in $La_2CuO_{4+\delta}$ and also with increasing concentration x per formula unit of Sr in $La_{2-x}Sr_xCuO_4$.

The system $La_{2-x}Sr_xCuO_4$ is of particular interest because it changes from an antiferromagnetic insulator to a superconductor to a nonsuperconductive metal on increasing x over the range $0 \leq x \leq 0.34$. Clearly, the superconductive phase appears at the crossover from localized-electron behavior in La_2CuO_4 to itinerant-electron behavior in $x \geq 0.3$. In the mixed-valent system, lattice instabilities associated with this crossover do not manifest themselves in a static CDW, but in a dynamic coupling to locally cooperative, dynamic oxygen displacements. Therefore, it is instructive to compare the properties of the $La_{2-x}Sr_xCuO_4$ system with those of the $La_2CuO_{4+\delta}$ system where the O_i atoms are mobile.

Following the procedure of Wattiaux et al. [23] and Grenier et al. [24], we were able to oxidize $La_2CuO_{4+\delta}$ electrochemically to $\delta=0.1$ [25]. A high O_i mobility at room temperature insured homogeneity of the oxygen stoichiometry within a few days. Although we obtained a $\delta=0.054$ sample at room temperature, we found it difficult to vary δ by small steps in the range $0.05 < \delta < 0.07$; samples in this region were oxidized quickly to $\delta=0.07$, which appears to be close to the O_i order–disorder boundary δ_0. As shown in the resulting phase diagram of Fig. 1, the orthorhombic–tetragonal transition temperature T_t decreases with increasing δ in the compositional range $0 \leq \delta \leq 0.034$ and it increases with δ for $\delta \geq 0.07$ at T_t' where the orthorhombic distortion appears to be due to an ordering of the O_i atoms in the interstitial sites of the $(LaO)_2$ layers; the distortion below T_t' is not due to a cooperative tilting of the CuO_6 octahedra that relieves the compressive stress on the CuO_2 sheets.

It was recognized early that compositions with $\delta \approx 0.03$, obtained by slow cooling La_2CuO_4 in air at atmospheric pressure, phase segregate at room temperature into an antiferromagnetic phase and a filamentary superconductive phase [26, 27]. Chaillot et al. [28] showed, with neutron-diffraction data, that the phase boundary of the antiferromagnetic phase is very close to the parent composition with $\delta=0.0$. With this phase boundary, we were able to map out the temperature T_s below which the spinodal phase segregation occurs. This classical phase segregation occurs because the O_i atoms remain mobile down to 200 K. Monitoring of the temperature dependence of the resistivity and thermoelectric power in both $La_2CuO_{4+\delta}$ and $La_{2-x}Sr_xCuO_4$ [25, 29] has shown that in both systems there is a change at room temperature from large (approximately 5 Cu centers) single-hole polarons to multihole polarons for $\delta<0.05$ and for $x<0.10$. This matching of the limiting hole concentration for the underdoped (single-hole polarons at room temperature)

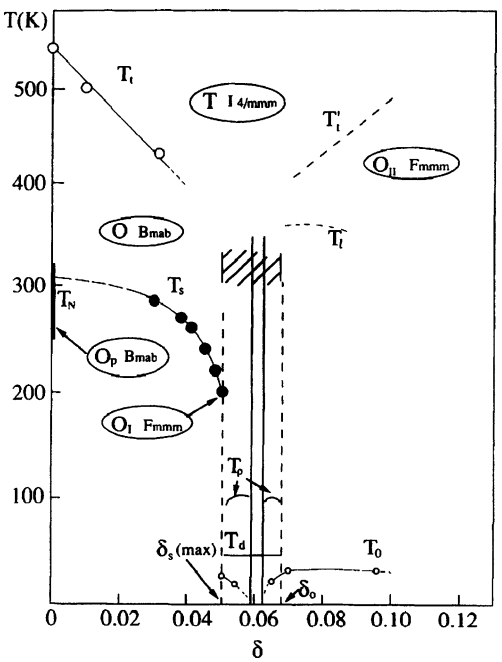

Fig. 1 Phase diagram for $La_2CuO_{4+\delta}$. O_i atoms are mobile to 200 K at δ_s(max). T_N is parent-phase Néel temperature and T_ρ marks onset of dynamic phase segregation (charge fluctuations) in the $\delta=0.07$ superconductive phase. T_l marks a transition from a polaron liquid to a polaron-gas in the superconductive phase and T_o is the zero-resistance temperature. A transport anomaly at T_d is associated with the $p=1/8$ competitive phase, after [25]

compositional range shows that the O_i atoms each capture two electrons to become, formally, O_i^{2-} ions.

The observation of an unstable oxygen content in the interval $0.05 < \delta < 0.07$ is significant; it signals that, once multihole polarons form, they order into a single, superconductive phase stable in the range $0.07 \leq \delta \leq 0.10$, corresponding to the single superconductive phase in the range $0.14 \leq x \leq 0.20$ in $La_{2-x}Sr_xCuO_4$. Since the increase in T_t' with δ in the range $0.07 \leq \delta \leq 0.10$ shows that the O_i order at δ=0.07 is not optimal, it is reasonable to conclude that the driving force for the room temperature uptake of oxygen in the interval $0.05 \leq \delta \leq 0.07$ is at least partially due to the stability of a peculiar multihole-polaron phase that becomes superconductive at low temperatures. The mobility of the O_i atoms at room temperature thus reinforces the conclusion that the superconductive phase is a thermodynamically distinguishable phase [29].

In the underdoped range $0 \leq \delta \leq 0.05$, the single-hole polarons remain isolated at room temperature, but below T_s; a spinodal phase segregation into a parent hole-free phase and a phase containing multihole polarons shows that, below room temperature, the phase with large single-hole polarons is not stable; it segregates into a parent phase and a phase containing a specific concentration of multihole polarons within a parent-phase matrix. In the $La_{2-x}Sr_xCuO_4$ system, there are no mobile ions for a classic phase segregation; but the transport data indicate locally cooperative oxygen displacements condense multihole polarons in a phase that is distinguishable from the parent phase [29].

A recent careful investigation of the critical composition for the onset of superconductivity in the $La_{2-x}Sr_xCuO_4$ system has shown that superconductivity appears abruptly with a finite T_c within the multihole-polaron phase at a critical hole concentration x_c=0.054 [30].

Tranquada et al. [31, 32] have shown that where $La_{2-x}Ba_xCuO_4$ undergoes a second structural change to a low-temperature tetragonal phase, the multihole polarons condense at x=1/8 into pinned metallic stripes containing a 50–50 Cu(II)–Cu(III) formal mixed valence separated by parent-phase magnetic-insulator slabs. This unusual static CDW shows a clear segregation into itinerant-electron and localized-electron regions as a result of locally cooperative oxygen displacements; it represents a phase that, in the range $0.05 < \delta < 0.07$, competes with the superconductive phase in which unpinned multihole polarons remain mobile. In the absence of a structural change that pins the metallic stripes, as is the case in $La_2CuO_{4+\delta}$ and $La_{2-x}Sr_xCuO_4$, this competition lowers but does not suppress T_c in the neighborhood of δ=0.0625 and x=1/8.

Daou et al. [33] have subjected the superconductive phase to a high magnetic field to quench the superconductivity; this experiment revealed the presence of a QCP beneath the superconductive phase at $x \approx 1/6$ and a linear temperature dependence of the resistivity characteristic of polaronic conduction with a motional enthalpy $\Delta H_m \approx 0$.

I have argued elsewhere [34] that the superconductive phase contains two-hole polarons covering four Cu centers with a 50–50 Cu(II)–Cu(III) formal mixed valence; the two electrons within a polaron occupy molecular orbitals and are spin-paired. These mobile bosons are separated by electrostatic forces in a matrix of Cu(II) ions with localized electrons. The two-hole polarons are stabilized by locally cooperative oxygen displacements, and the associated elastic and electrostatic energies are minimized by an ordering of the bipolarons. Coupling of an ordered, mobile array of bosonic polarons to optical phonons would give rise to superconductivity.

Conclusions

The examples cited lead to the following conclusions:

1. The first-order character of the transition from localized to itinerant 3d-electron behavior in transition-metal oxides has been demonstrated not only for cation–cation interactions, but also for cation–anion–cation interactions between like atoms.
2. At crossover, CDWs provide an ordered segregation between strong and weak interatomic interactions; the ordering maximizes the gain in bond energy while minimizing the loss in elastic energy.
3. The lattice instabilities manifest in a CDW may be found either on the approach to crossover from the localized-electron side or from the itinerant-electron side; they need not be triggered by introducing a change in lattice periodicity that introduces a gap at the Fermi energy of a narrow-band metal.
4. At crossover, single-valent compounds with transition-metal cation–cation interactions form an ordered array of cation clusters in which the short cation–cation bonds normally each contain an electron-pair bond as in the dimers of VO_2 and the trimers of $LiVO_2$; but single-electron bonds rather than electron-pair bonds are possible as in the dimer chains of $Zn[V_2]O_4$ where crossover in the [011] and [101] directions is approached from the localized-electron side by ordering of a localized electron in the *xy*-orbital in the basal plane. Below 260 K, the spinel $Mg[Ti_2]O_4$ forms isolated Ti–Ti dimers bonded by electron pairs [35]. Three-electron cation–cation bonding is also known, particularly in Fe(II) sulfides where the majority-spin electrons are localized, but the minority-spin electrons become delocalized [36].
5. At crossover, single-valent compounds with cation–anion–cation interactions form an ordered array of strong

cation–anion bonding in a polyanion cluster separated by like cations having localized *3d*-electrons. Formation of polyanion clusters may result in a disproportionation reaction as is found with $2\,Fe(IV) = Fe(V) + Fe(III)$ [37], but $HoNiO_3$ shows that charge disproportionation need not occur; in this perovskite, low-spin $Ni(III)O_6$ polyanions are separated by low-spin Ni(III) ions with a localized t^6e^1 configuration that gives a large local Jahn-Teller site distortion.

6. Insertion compounds containing mobile guest ions, as is the case with $La_2CuO_{4+\delta}$, permits a unique way of monitoring the crossover in a mixed-valent compound. The mobility of the O_i^{2-} ions in $La_2CuO_{4+\delta}$ clearly reveals that the superconductive phase is a thermodynamically distinguishable phase in which multihole polarons are mobile in a hole-free matrix; this stable phase forms on cooling below room temperature. A logical deduction is that the multihole polarons are two-hole polarons covering four copper centers with an average formal Cu valence of 2.5+. The polarons are formed by locally cooperative oxygen displacements, and superconductivity appears where an ordered mobile array couples to optical-mode phonons. In this model, the bosonic polarons are kept apart by electrostatic coulomb repulsion, but electrostatic energy is gained by an ordering of the positively charged polarons in the negatively charged matrix at a specific concentration of polarons.
7. A lattice distortion that pins the polarons can cause the two-hole polarons to condense into an ordered array of itinerant-electron stripes and localized-electron slabs at a specific hole concentration, *viz* $x=1/8$ in $La_{2-x}Ba_xCuO_4$.
8. Application of a high magnetic field suppresses the superconductive phase to reveal it masks a QCP. The pressure dependence of the transport properties of $PrNiO_3$ has revealed that a first-order transition to QCP behavior at low temperatures is characteristic of the crossover from localized to itinerant electronic behavior.
9. A critical V–V separation R_c for the transition from localized to itinerant behavior of the *3d*-electrons of V (III) ions in octahedral sites sharing edges appears to be $2.92\ Å < R_c < 2.97\ Å$. An earlier study [35] of the ordered rock-salt $Li_2[V_2]O_4$ indicated an $R_c < 2.93\ Å$. These observations narrow the critical V–V separation to $R_c \approx 2.92\ Å \pm 0.02\ Å$.

References

1. Schöllhorn R (1982) Solvated intercalation compounds of layered chalcogenide and oxide bronzes. In: Whittingham MS, Jacobson AJ (eds) Intercalation chemistry. Academic, New York, pp 315–360
2. Goodenough JB (2002) Oxide cathodes. In: Schalkwijk WA, Scrosati B (eds) Advances in lithium-ion batteries. Kluwer Academic/Plenum, New York, pp 135–154
3. Goodenough JB (1984) The effective U in oxides and sulfides. In: Acrivos JV, Mott NF, Yoffe A (eds) NATO "Davy" ASI. Physics and chemistry of electrons and ions in condensed matter. Reidel, Dordrecht, pp 1–44
4. Anderson PW (1959) Phys Rev 115:2–13
5. Adler D, Brooks H (1967) Phys Rev 155:826–840
6. Goodenough JB (2001) Struct Bond 98:1–16
7. Bersuker GI, Goodenough JB (1997) Physica C 274:267–285
8. Morin FJ (1959) Phys Rev Lett 3:34–36
9. Andersson G (1956) Acta Chem Scand 10:623–630
10. Heckingbottom R, Linnett JW (1962) Nature 194:678
11. Kittel C (1996) Introduction to solid state physics, 7th edn. Wiley, New York, 300
12. Lomer WM (1962) Proc Phys Soc 80:489–496
13. Bongers PF (1957) Thesis. Univ. of Leiden, July 4
14. Pen HF, van den Brink J, Khomskii DI, Sawatzky GA (1997) Phys Rev Lett 78:1323–1326
15. Goodenough JB (1971) Prog Solid State Chem 5:145–399
16. Rogers DB, Arnott RJ, Wold A, Goodenough JB (1963) J Phys Chem Solids 24:347–360
17. Pardo V, Blanco-Canosa S, Rivadulla F, Khomskii DI, Baldomir D, Wu H, Rivas J (2008) Phys Rev Lett 101:256403-1–256403-4
18. Baldomir D, Pardo V, Blanco-Canosa S, Rivadulla F, Khomskii DI, Wu H, Piñeiro A, Arias JE, Rivas J (2009) J Mag Mag Mater 321:679–681
19. Goodenough JB (1967) Czech J Phys 17:304–336
20. Zhou JS, Goodenough JB (2004) Phys Rev B 69:153105-1–153105-4
21. Alonso JA, Martinez-Lope MJ, Casais MT, Garcia-Munoz JL, Fernandez-Diaz MT, Aranda MAC (2001) Phys Rev B 64:094102-1–094102-10
22. Zhou JS, Goodenough JB, Dabrowski B (2005) Phys Rev Lett 94:226602-1–226602-4
23. Wattiaux A, Park JC, Grenier JC, Pouchard M (1990) CR Acad Sci Ser II 310:1047–1054
24. Grenier JC, Lagueyte N, Wattiaux A, Doumerc JP, Dordor P, Etourneau J, Pouchard M, Goodenough JB, Zhou JS (1992) Physica C 202:209–218
25. Zhou JS, Chen H, Goodenough JB (1994) Phys Rev B 50:4168–4180
26. Grant PM, Parkin SSP, Lee VY, Engler EM, Ramirez MC, Vasquez JE, Lim G, Jacowitz RD, Greene RL (1987) Phys Rev Lett 58:2482–2485
27. Johnson DC DC, Stokes JP, Goshorn DP, Lewandowski JT (1987) Phys Rev B 36:4007–4010
28. Chaillaut C, Chenavas J, Cheong SW, Fisk Z, Marezio M, Morosin B, Schirber JE (1990) Physica C 170:87–94
29. Goodenough JB, Zhou JS, Chan J (1993) Phys Rev B 47:5275–5286
30. Takami T, Zhou JS, Cheng JG, Goodenough JB, Matsubayashi K, Uwatoko Y (2009) New J Phys 11:013057–013069
31. Tranquada JM, Sternlieb BJ, Axe JD, Nakamura Y, Uchida S (1995) Nature 375:561–563
32. Tranquada JM, Ichikawa N, Uchida S (1999) Phys Rev B 59:14712–14722
33. Daou R, Doiron-Leyraud N, LeBoeuf D, Li SY, Laliberté F, Cyr-Choinière O, Lo YJ, Balicas L, Yan JQ, Zhou JS, Goodenough JB, Taillefer L (2008) Nat Phys 5:31–34
34. Goodenough JB (2003) J Phys Condens Matter 15:R257–R326
35. Schmidt M, Ratcliff W II, Radaelli PG, Refson K, Harrison NM, Cheong SW (2004) Phys Rev Lett 92:056402-1–056402-4
36. Goodenough JB (1982) Ann Chim 7:489–504
37. Battle PD, Gibb TC, Nixon S (1989) J Solid State Chem 79:75–85